Pseudomonas aeruginosa PA14 biofilms produce R-bodies, extendable protein polymers with roles in host colonization and virulence

Bryan Wang[1], Yu-Cheng Lin[1], Jeanyoung Jo[1], Alexa Price-Whelan[1], Shujuan Tao McDonald[1,2], Lewis M. Brown[1,2], and Lars E.P. Dietrich[1]*

1Department of Biological Sciences, Columbia University, New York, NY, USA

[2]Quantitative Proteomics and Metabolomics Center, Columbia University, New York, NY, USA

*email: LDietrich@columbia.edu

reb genes code for R-bodies: large, extendable polymers that are known for their roles in obligate endosymbioses. In the non-endosymbiotic pathogen _Pseudomonas aeruginosa_, _reb_ homologues are part of a cluster found in virulent strains. Here, we demonstrate that R-bodies are produced in abundance by _P. aeruginosa_ PA14 subpopulations during biofilm growth, identify regulators of _reb_ gene expression, and show that _reb_ genes are required for full colonization and virulence in host models.

R-bodies are enigmatic biological machines that have been characterized most extensively in *Caedibacter taeniospiralis*, an obligate endosymbiont of paramecia. These structures are composed of ~ 12 kDa monomers that polymerize to form hypercoiled ribbons ~ 0.5 µm in diameter [1]. In response to changes in parameters such as pH, temperature or ionic strength [2–4], R-body coils extend into 10-20-µm-long needle-like structures (i.e., ~ 10X the length of the producing cell), lysing the bacterium [4,5]. In the *Caedibacter-Paramecium* endosymbiosis, R-body-mediated lysis is thought to release an unidentified factor that is toxic to other paramecia. R-body-producing endosymbionts therefore confer onto their host cell a “killing” phenotype and a competitive advantage against naive peer cells, a phenomenon that was first described by Tracy M. Sonneborn in 1938 [6].

Diverse proteobacterial genomes contain homologues to genes for R-bodies (i.e., *reb* genes) [7]. In the opportunistic pathogen *P. aeruginosa*, *reb* gene homologues are part of a cluster that is conserved in a substantial fraction (147/241) of complete strain genomes, including those of the virulent strains PA14 and LESB58, but that is not present in the popular and notably less-virulent model strain PAO1 [8,9] (Supplementary File 1). We will refer to genes in the *P. aeruginosa* PA14 *reb* cluster using names shown in **Figure 1a**, which are based on a prior study [10] and phylogenetic analyses conducted using the *C. taeniospiralis* structural genes for R-body production (**Supplementary Figure 1**). Included in this conserved locus are two regulatory

genes, *rebZ* and *fecI2*, which code for a transcription factor and sigma factor, respectively, and which in a prior study were required for full virulence in a *C. elegans* killing assay [9] (**Figure 1a**). Via bioinformatic analyses, we found that though *reb* structural gene homologues are scattered across the phylogenetic tree of the genus *Pseudomonas* **(Supplementary Figure 2)**, homologues of the regulatory genes show strong conservation in strains that contain *reb* structural genes, both within the species *P. aeruginosa* (in 146/147 *reb* homologue-containing genomes; **Supplementary Table 1**) and among other pseudomonads (**Figure 1a, Supplementary Figure 2**). Though all of these observations hinted at a potential role for R-bodies in *P. aeruginosa*-host associations, R-body production by *P. aeruginosa* biofilms and during host colonization had not been investigated.

To examine whether PA14 produces R-bodies, we applied a modified R-body enrichment protocol [11] to biofilms formed by the WT and by Δ*pel*, a mutant that is unable to produce the major PA14 exopolysaccharide and yields biofilms that are more amenable to disruption. We performed protein mass spectrometry (MS) and scanning-electron microscopy (SEM) on the isolated SDS-insoluble fractions (**Figure 1b**). Products of the *reb* cluster were detected by MS. Three products—PA14_27680, RebP1, and RebP2-- were detected at similar levels and were among the 12 most abundant proteins in our sample (**Figure 1c**). RebP1 and RebP2 have 40-42% and 34-40% homology, respectively, to RebB and RebA from *C. taeniospiralis,* which constitute the main structural components of R-bodies in that organism [12]. *PA14_27680* is conserved in all pseudomonads that contain at least one *reb* structural gene, suggesting that it may encode another R-body structural component. One other uncharacterized protein coded for by the *reb* gene cluster, PA14_27675, was also detected in the SDS-insoluble fractions (**Supplementary File 2 and Figure 1c**). Consistent with the MS results, our SEM analyses revealed the presence of R-bodies in preparations from WT PA14 biofilms (**Figure 1d**). We detected R-bodies in various states of extension ranging from hypercoiled (~ 450 nm long) to

fully extended (~ 5.5 μm long) (**Figure 1d, e**). These structures were not observed in a deletion mutant lacking the *rebP1P2* operon (Δ*rebP1P2*) (**Supplementary Figure 3**). Taken together, these data indicate that R-bodies are produced by PA14 biofilms.

Based on the conservation of *rebZ* and *fecI2* in strains containing R-body structural gene homologues (**Figure 1a; Supplementary File 1; Supplementary Figure 1**), we reasoned that one or both of these genes control expression of *rebP1P2*. To test this, we generated constructs that report expression from the *rebP1P2* promoter (P_{rebP1}) as red (mScarlet) or green (GFP) fluorescence and inserted these into a neutral site on the chromosome in WT PA14 and regulatory gene mutants. We observed P_{rebP1} activity in WT colony biofilms that was dependent on the presence of both *rebZ* and *fecI2* (**Figure 1f-h** and **Supplementary Figure 3**). Because biofilm development leads to the formation of steep chemical gradients that can affect gene expression patterns along the z-axis [13], we wanted to visualize P_{rebP1} activity across depth. We employed a thin sectioning protocol to prepare vertical sections taken from the center region of three-day-old colony biofilms [14]. Confocal microscopy of P_{rebP1}-*mScarlet* biofilm sections revealed that, strikingly, cells expressing *rebP1P2* are present in thin striations such that both bright and dark cells are situated at the same depth. For comparison, we prepared sections of biofilms in which *gfp* expression was driven by a constitutive promoter ($P_{PA1/04/03}$-*gfp*) and observed fluorescence that is more consistent between cells at the same depth (**Supplementary Figure 3**). Our results suggest that P_{rebP1}-driven expression is stochastic and that expression status is heritable during vertical growth in the the biofilm.

The fact that homologues of the *C. taeniospiralis* R-body structural genes are found in diverse free-living bacteria suggests that their roles extend beyond endosymbiotic interactions [7] (**Supplementary Figure 1**). *P. aeruginosa* forms biofilms and acts as an extracellular pathogen during colonization of a range of hosts including plant and nematode models [15,16]. To examine

whether *rebP1P2* is expressed during interactions with hosts, we employed the P_{rebP1}-*mScarlet* reporter strain in *Arabidopsis thaliana* seedling and *Caenorhabditis elegans* gut colonization assays. In both hosts, as in biofilms, *rebP1P2* expression patterns were distinct from those exhibited by a promoter driving constitutive expression of mScarlet ($P_{PA1/04/03}$-*mScarlet*). While constitutive mScarlet production was uniform and fuzzy across colonized regions of hosts (**Figure 2a, b**), *rebP1P2* expression was punctate and restricted to a subset of PA14 cells (**Figure 2a**, **b**). To rule out the possibility that constitutive mScarlet production represented non-specific, background fluorescence, we expressed mScarlet without a promoter (MCS-*mScarlet*) in these hosts. Indeed, promoterless mScarlet expression was not observed in either *A. thaliana* or *C. elegans* (**Figure 2a, b**). The distinct *rebP1P2* expression patterns we observed in the colony biofilm and host contexts may indicate that there is an advantage to restricting R-body production to a subset of cells in the population.

In *C. taeniospiralis* and *Azorhizobium caulinodans*, R-body production has been linked to host-associated phenotypes that confer toxicity [4,17,18]. We hypothesized that R-bodies contribute to PA14 host colonization and/or pathogenicity and therefore performed established assays to test such contributions of PA14 R-body production in our two host systems. In *A. thaliana*, we quantified the extent to which PA14 WT and mutant strains colonized seedlings after inoculation and five days of plant growth. For the *C. elegans* virulence assay, we quantified percent survival for up to four days after synchronized populations of worms were exposed to PA14 WT and mutant strains. When compared to WT PA14, Δ*rebP1P2* displayed attenuated host colonization (**Figure 2e**) and virulence (**Figure 2f**); both phenotypes were restored to WT levels upon complementation of *rebP1P2*.

In many hosts and various infection sites in humans, biofilm formation is critical to bacterial colonization and virulence and requires production of matrix [19]. Matrix secretion is a defining

feature of biofilms; the matrix functions as the "glue" that holds bacterial cells together and can facilitate attachment to the host [20]. To test whether matrix production is affected by a defect in R-body production, we examined biofilm development using a standardized colony morphology assay, in which the dye Congo red is provided in the medium and binds to biofilm matrix. We found that matrix production and biofilm development were unaltered in the Δ*rebP1P2* mutant (**Figure 2c**). Furthermore, Δ*rebP1P2* showed no fitness disadvantage when grown in mixed-strain colony biofilms with the WT parent (**Figure 2d**). We conclude the *A. thaliana* colonization and *C. elegans* killing defects observed in the Δ*rebP1P2* mutant are not mediated via effects on biofilm formation and that the benefit of R-body production is specific to the host-associated lifestyle.

We have shown here the production of R-bodies by PA14 cells growing in biofilms and demonstrated a role for these structures during host infection. Expression of the PA14 R-body structural genes is stochastic and can be observed both in independent biofilms and during association with hosts. However, an advantage to R-body production is detectable only during host colonization, suggesting that R-body function is specific to infection. *Caedibacter* R-body extension is triggered by low pH and occurs in phagosomes of naive paramecia, prompting *Caedibacter* lysis and the release of other toxins within *Caedibacter* cells and thereby killing the eukaryotic predator [4,5]. We speculate that PA14 R-body extension is similarly triggered in a host-specific manner and that cells in the R-body-producing subpopulation act as "kamikazes" to release other bacterial products that facilitate colonization and enhance virulence. Our findings identify R-bodies as novel *P. aeruginosa* virulence factors and raise the possibility that R-body production contributes to the behaviors of diverse free-living bacteria during interactions with other organisms.

METHODS

Bacterial strains and growth conditions. Strains used in this study are listed in Supplementary Table 1. Liquid cultures of *Pseudomonas aeruginosa* strain UCBPP-PA14 (PA14) were grown in lysogeny broth (LB) at 37˚C with shaking at 250 rpm. Biological replicates were inoculated from distinct clonal-source colonies grown on LB + 1.5% agar plates. Overnight precultures were grown for 14-16 h and subcultures were prepared by diluting precultures 1:100 in LB and growing until mid-exponential phase (OD at 500 nm ~ 0.5).

Construction of PA14 mutant strains. Markerless deletion, complementation, and constitutive-expression strains were made as described previously [21]. Briefly, flanking sequences containing the target locus were amplified using the primers listed in Supplementary Table 2 and inserted into pMQ30 through gap repair cloning in *Saccharomyces cerevisiae* InvSc1 [22]. Each plasmid, listed in Supplementary Table 3, was moved into PA14 and resolved out using selective media. PA14 double recombinants (markerless strains) were confirmed by PCR.

Construction of PA14 reporter strains. The desired promoter region (500 bp upstream of the *rebP1P2* operon for $P_{rebP1P2}$-*mScarlet*; the synthetic *lac* promoter for $P_{PA1/03/04}$-*mScarlet*) was amplified using the primers listed in Supplementary Table 1 and ligated into pLD3208, upstream of *mScarlet*. Resulting plasmids were integrated into a neutral site in the PA14 genome using biparental conjugation and the plasmid backbone was resolved out via FLP-FRT recombination. Reporter constructs containing *mScarlet* were isolated using selective media and confirmed by PCR.

Colony biofilm morphology assays. Ten µL of liquid subcultures were spotted on 60 mL of colony morphology medium (1% tryptone, 1% agar, 40 µg/mL Congo red dye, 20 µg/mL

Coomassie blue dye) and incubated for up to five days in the dark at 25˚C with >90% humidity (Percival CU-22L) and imaged daily with an Expression 11000XL scanner (Epson). Images shown are representative of at least six biological replicates.

Competition assays. Fluorescent, mScarlet-expressing and non-fluorescent cells were mixed together in a 1:1 ratio from subcultures and grown as mixed-strain biofilms as described above. After three days, biofilms were resuspended in 1 mL of 1% tryptone and homogenized in a bead mill homogenizer (Omni Bead Ruptor 12) for 99 s on the “high” setting. Serial dilutions of homogenized cells were plated onto 1% tryptone + 1.5% agar plates for colony forming unit (CFU) determination. Fluorescent CFUs were determined by imaging with a Typhoon FLA7000 fluorescent scanner (GE Healthcare).

Purification of SDS-insoluble biofilm fraction. Twenty, five-day-old PA14 Δ*pelB-G* colony biofilms were resuspended in 80 mL of sterile phosphate-buffered saline (PBS) and sonicated for 2 x 10 s on ice with the microtip of a Sonifier 250 (Branson). SDS and β-mercaptoethanol were added to final concentrations of 2% and 5%, respectively. After nutating on a Nutating Mixer (Fisher Scientific) at room temperature (RT; ~ 25˚C) for 60 min, the sample was aliquoted into 1.5-mL microfuge tubes and the insoluble fraction was spun down at 16,873 x g for 5 min. The supernatant was discarded and pellets were pooled together.

Mass spectrometry of SDS-insoluble proteins. The SDS-insoluble pellet was washed three times with Optima water (Fisher Scientific), solubilized in 100 µL of 98% formic acid at room temperature for 1 h. spin-vacuum dried for 1.5 h, washed with 50% methanol and water, and then dissolved in 2% RapiGest (Waters Corp.) with 6 mM DTT. Samples were then sonicated, boiled, cooled, cysteines reduced and alkylated and proteins digested with trypsin as described previously [23]. Liquid Chromatography mass/ spectrometry (120 min runs) was performed with

the Synapt G2 (Waters Corp.) in positive resolution/ion mobility mode with proteins identified with ProteinLynx Global Server (PLGS) as described previously [24]. Proteins were also identified and semi-quantitatively measured with a Q Exactive HF (Orbitrap, Thermo Scientific) with Mascot V. 2.5 as described previously [25]. Identification of the most abundant proteins in these preparations by the Q Exactive HF were confirmed by the qualitative orthogonal method (Synapt G2 ion mobility/PLGS analysis). The reference proteome UP000000653 for *Pseudomonas aeruginosa* strain PA14 from UniProt (Release 2015_10, 11/10/2015) was used for all database searches. All raw MS data files will be publicly available at the MassIVE data repository (https://massive.ucsd.edu).

Scanning-electron microscopy. The SDS-insoluble pellet was resuspended in pre-fixative solution (2% paraformaldehyde, 2.5% glutaraldehyde, 0.0075% L-lysine in PBS), nutated at RT for 30 min in the dark, washed in PBS, and fixed in 2.5% glutaraldehyde in PBS at RT for 30 min in the dark. Fixed pellets were washed twice in PBS, dehydrated through a series of 60-min ethanol washes (25%, 50%, 75%, 95%, 3 x 100%) and visualized with a Helios NanoLab DualBeam 660 (FEI).

Fluorescence visualization in *P. aeruginosa* colony biofilms. For whole-colony fluorescence imaging, colony biofilms were grown as described for morphology assays but on growth medium without dyes. After three days, bright field images and fluorescence images were visualized with a Zeiss Axio Zoom.V16 fluorescence stereo zoom microscope. Thin sections of colony biofilms ($n \geq 3$ biological replicates) were prepared as described previously [14]. Differential interference contrast (DIC) and fluorescent confocal images were captured using an LSM800 confocal microscope (Zeiss).

220 ***A. thaliana* colonization assays.** *Arabidopsis thaliana* ecotype Columbia (Col-0) seeds were sterilized using standard bleach protocols [26]. Washed, surface-sterilized seeds were resuspended in 0.1% agar and subjected to 24 h of cold treatment at 4˚C, then plated and germinated on half-strength MS agar medium containing Gamborg vitamins [27]. Seeds were incubated at 22˚C with a 12-h-light/12-h-dark photoperiod (100-150 μE/m^2/s; Percival CU-22L) 225 for three weeks. *A. thaliana* seedlings were then inoculated with PA14 using a flood inoculation assay [28] and incubated under the same light/dark conditions for five days. For visualization of PA14-infected *A. thaliana*, leaves were excised and *mScarlet* fluorescence was visualized with a Zeiss Axio Zoom.V16 fluorescence stereo zoom microscope. For quantification of PA14 colonization of *A. thaliana*, seedlings were harvested, weighed, and surface-sterilized with 1 mL 230 of 5% H_2O_2 in water for 3 min. These seedlings were washed five times with sterile PBS and homogenized in 1 mL of PBS in a bead mill homogenizer on the “high” setting for 99 sec. Serial dilutions of homogenized tissue were plated onto LB agar plates containing 4 μg/ml tetracycline and grown overnight at 37°C to select for *P. aeruginosa*, and CFU counts were quantified.

235 ***C. elegans* pathogenicity assays.** Ten μL of overnight PA14 cultures were spotted onto NGM agar plates [29] and incubated at 24 h at 37˚C, followed by 48 h at 25˚C. Thirty to 35 larval stage 4 (L4) worms were picked onto the PA14-seeded plates and incubated at 25˚C. For visualization of PA14-infected worms, worms were exposed to PA14 for three days, immobilized in 10 mM levamisole in water, mounted on a 2% agarose pad on a glass slide, and imaged at 40x on a 240 Zeiss Axio Imager D1 epifluorescence microscope with an AxioCam Mrm. For pathogenicity killing assays, which were modified from Tan 1999, live/dead worms were counted for up to four days after plating onto PA14-seeded plates. *unc-44*(*e362*) worms, which exhibit body movement deficits, were used instead of wild-type to prevent worms from crawling off the plates.

Phylogenetic analysis. Trees in Supplementary Figures 1 and 2 were generated with Geneious Prime 2020.2.4 using Muscle for sequence alignment and the neighbor-joining method for tree building (genetic distance model: Jukes-Cantor).

ACKNOWLEDGEMENTS

This study was supported by NIH/NIAID grant R01AI103369, an NSF CAREER award to L.E.P.D., and NSF GRFP grant DGE - 1644869 to B.W. Mass spectrometer acquisition and operations were funded by New York State Stem Cell Science Board (NYSTEM contracts CO2361 and C029159) with matching funds from Columbia University and the Columbia Stem Cell Initiative (LMB). We thank Jason Reed (UNC Chapel Hill) for providing *A. thaliana* Col-0 seeds, Hillary Callahan (Barnard College) for technical support in growing seedlings, Martin Chalfie for provision of *C. elegans unc-44(e362)*, and Iva Greenwald for technical support with imaging of *C. elegans*. We also thank Zarina Akbary for technical assistance in creating the Δ*rebZ*Δ*fecI2* P_{rebP1}-*gfp* strain.

REFERENCES

1. Quackenbush, R. L. & Burbach, J. A. Cloning and expression of DNA sequences associated with the killer trait of Paramecium tetraurelia stock 47. *Proc. Natl. Acad. Sci. U. S. A.* **80**, 250–254 (1983).
2. Gibson, I. A comparison of the refractile bodies (R-bodies) of certain bacteria—III. Nucleotide sequence homologies and R-body function. *Micron and Microscopica Acta* **15**, 253–259 (1984).
3. Gibson, I., Bedingfield, G., Dobbs, H. & Shackleton, J. Effects of various agents on the R bodies of certain bacteria. *Micron and Microscopica Acta* **18**, 71–75 (1987).
4. Pond, F. R., Gibson, I., Lalucat, J. & Quackenbush, R. L. R-body-producing bacteria. *Microbiol. Rev.* **53**, 25–67 (1989).
5. Jurand, A., Preer, J. R. & Rudman, B. M. Further investigations on the prelethal effects of the killing action of kappa containing killer stocks ofParamecium aurelia. *J. Exp. Zool.* **206**, 25–47 (1978).
6. Sonneborn, T. M. Mating Types in Paramecium Aurelia: Diverse Conditions for Mating in Different Stocks; Occurrence, Number and Interrelations of the Types. *Proc. Am. Philos. Soc.* **79**, 411–434 (1938).
7. Raymann, K., Bobay, L.-M., Doak, T. G., Lynch, M. & Gribaldo, S. A genomic survey of Reb homologs suggests widespread occurrence of R-bodies in proteobacteria. *G3* **3**, 505–516 (2013).
8. Winsor, G. L. *et al.* Enhanced annotations and features for comparing thousands of Pseudomonas genomes in the Pseudomonas genome database. *Nucleic Acids Res.* **44**, D646-53 (2016).
9. Feinbaum, R. L. *et al.* Genome-wide identification of Pseudomonas aeruginosa virulence-related genes using a Caenorhabditis elegans infection model. *PLoS Pathog.* **8**, e1002813

(2012).

10. Schulz, S. *et al.* Elucidation of sigma factor-associated networks in Pseudomonas aeruginosa reveals a modular architecture with limited and function-specific crosstalk. *PLoS Pathog.* **11**, e1004744 (2015).
11. Polka, J. K. & Silver, P. A. A Tunable Protein Piston That Breaks Membranes to Release Encapsulated Cargo. *ACS Synth. Biol.* **5**, 303–311 (2016).
12. Heruth, D. P., Pond, F. R., Dilts, t. J. A. & Quackenbush, R. L. Characterization of Genetic Determinants for R Body Synthesis and Assembly in Caedibacter taeniospiralis 47 and 116. *J. Bacteriol.* **176**, 3559–3567 (1994).
13. Stewart, P. S. & Franklin, M. J. Physiological heterogeneity in biofilms. *Nat. Rev. Microbiol.* **6**, 199–210 (2008).
14. Cornell, W. C. *et al.* Paraffin Embedding and Thin Sectioning of Microbial Colony Biofilms for Microscopic Analysis. *J. Vis. Exp.* (2018) doi:10.3791/57196.
15. Tan, M. W., Mahajan-Miklos, S. & Ausubel, F. M. Killing of Caenorhabditis elegans by Pseudomonas aeruginosa used to model mammalian bacterial pathogenesis. *Proc. Natl. Acad. Sci. U. S. A.* **96**, 715–720 (1999).
16. Walker, T. S. *et al.* Pseudomonas aeruginosa-plant root interactions. Pathogenicity, biofilm formation, and root exudation. *Plant Physiol.* **134**, 320–331 (2004).
17. Preer, J. R., Jr, Preer, L. B. & Jurand, A. Kappa and other endosymbionts in Paramecium aurelia. *Bacteriol. Rev.* **38**, 113–163 (1974).
18. Matsuoka, J.-I. *et al.* A putative TetR-type transcription factor AZC_3265 from the legume symbiont Azorhizobium caulinodans represses the production of R-bodies that are toxic to eukaryotic cells. *Soil Sci. Plant Nutr.* **63**, 452–459 (2017).
19. Flemming, H.-C. *et al.* Biofilms: an emergent form of bacterial life. *Nat. Rev. Microbiol.* **14**, 563–575 (2016).
20. Donlan, R. M. Biofilms: microbial life on surfaces. *Emerg. Infect. Dis.* **8**, 881–890 (2002).

21. Okegbe, C. *et al.* Electron-shuttling antibiotics structure bacterial communities by modulating cellular levels of c-di-GMP. *Proc. Natl. Acad. Sci. U. S. A.* **114**, E5236–E5245 (2017).

22. Shanks, R. M. Q., Caiazza, N. C., Hinsa, S. M., Toutain, C. M. & O'Toole, G. A. Saccharomyces cerevisiae-based molecular tool kit for manipulation of genes from gram-negative bacteria. *Appl. Environ. Microbiol.* **72**, 5027–5036 (2006).

23. Oswald, E. S., Brown, L. M., Bulinski, J. C. & Hung, C. T. Label-free protein profiling of adipose-derived human stem cells under hyperosmotic treatment. *J. Proteome Res.* **10**, 3050–3059 (2011).

24. Yang, W. S. *et al.* Regulation of ferroptotic cancer cell death by GPX4. *Cell* **156**, 317–331 (2014).

25. Wobma, H. M. *et al.* The influence of hypoxia and IFN-γ on the proteome and metabolome of therapeutic mesenchymal stem cells. *Biomaterials* **167**, 226–234 (2018).

26. Clough, S. J. & Bent, A. F. Floral dip: a simplified method forAgrobacterium-mediated transformation ofArabidopsis thaliana. *The Plant Journal* vol. 16 735–743 (1998).

27. Murashige, T. & Skoog, F. A Revised Medium for Rapid Growth and Bio Assays with Tobacco Tissue Cultures. *Physiologia Plantarum* vol. 15 473–497 (1962).

28. Ishiga, Y., Ishiga, T., Uppalapati, S. R. & Mysore, K. S. Arabidopsis seedling flood-inoculation technique: a rapid and reliable assay for studying plant-bacterial interactions. *Plant Methods* **7**, 32 (2011).

29. Brenner, S. The genetics of Caenorhabditis elegans. *Genetics* **77**, 71–94 (1974).

30. Rahme, L. G. *et al.* Use of model plant hosts to identify Pseudomonas aeruginosa virulence factors. *Proc. Natl. Acad. Sci. U. S. A.* **94**, 13245–13250 (1997).

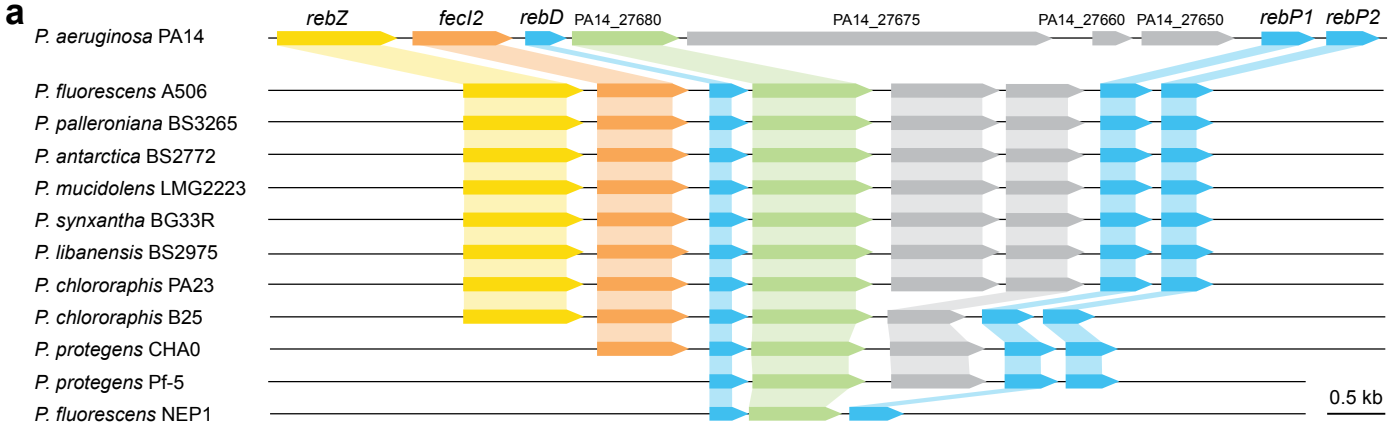

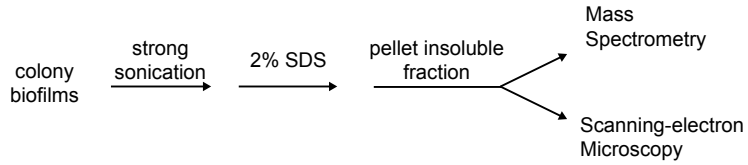

c

Protein Name	Locus (PA14/ PAO1)	Semiquantitative abundance WT	Semiquantitative abundance *Δpel*
HsiB2	PA14_43040/ PA1657	0.7	11.0
OprF	PA14_41570/ PA1777	6.8	10.4
OprL	PA14_51710/ PA0973	4.3	9.4
-	PA14_06990/ PA0537	1.5	8.4
HsiB3	PA14_34070/ PA2365	0.4	5.0
HsiC2	PA14_43030/ PA1658	0.5	4.9
HsiC3	PA14_34050/ PA2366	1.7	3.8
-	PA14_50740/ PA1053	1.9	2.6
-	**PA14_27680**	**0.6**	**2.1**
RebP2	**PA14_27630**	**0.8**	**1.4**
RebP1	**PA14_27640**	**0.8**	**1.4**
AlgP	PA14_69370/ PA5253	0.2	1.3

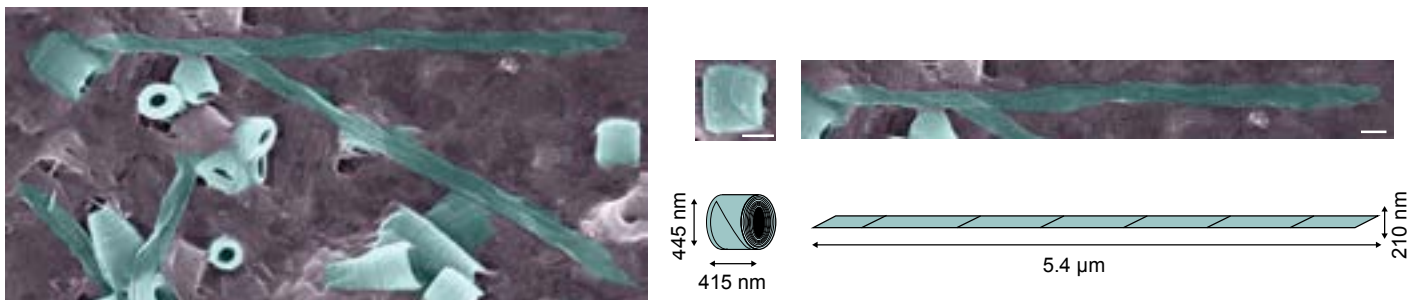

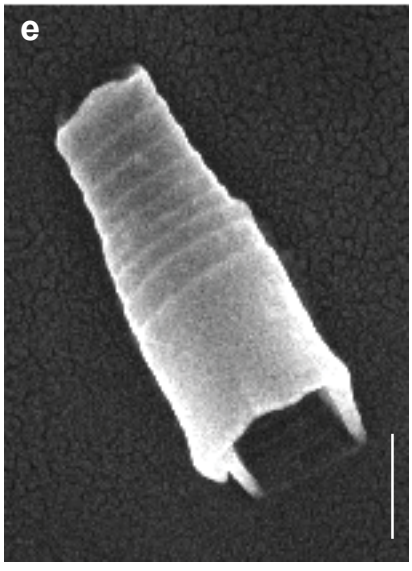

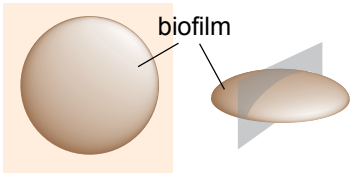

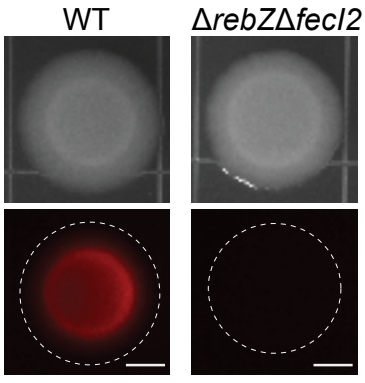

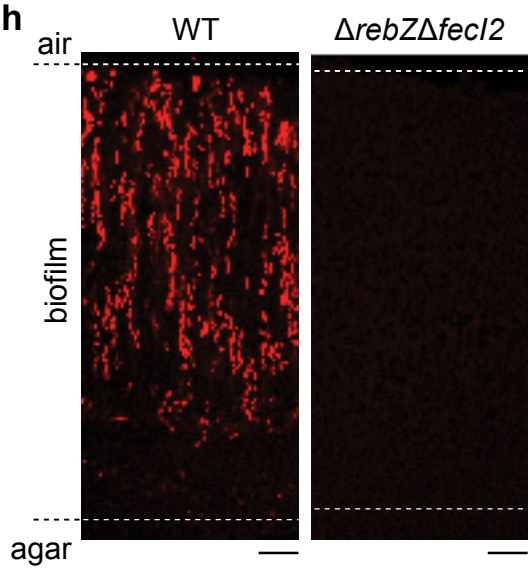

Fig.1. Components of the *reb* gene cluster, which are found in diverse pseudomonads, support R-body production by *Pseudomonas aeruginosa* PA14 biofilms. a, Chromosomal arrangement of genes associated with R-body production in representative *Pseudomonas* species and strains. Regulatory genes are shaded yellow and orange. Genes shaded blue are homologous to the R-body structural genes from *C. taeniospiralis*. *PA14_27680* and its homologues, which may code for a novel R-body component, are shaded green. **b,** Schematic showing method for preparation of SDS-insoluble material from PA14 biofilms. **c,** Top 12 most abundant proteins (semi-quantitative) detected in the SDS-insoluble formic acid solubilized fraction of WT (one replicate) and Δ*pel* (two biological replicates) by mass spectrometry. **d,** Left panel: Scanning-electron micrograph (SEM) image of R-bodies (false-colored turquoise) in the insoluble fraction. Scale bar = 1 μm. Right: SEM images, cartoon representations, and dimensions of individual selected R-bodies in fully coiled and fully extended states. Scale bars = 250 nm. **e,** SEM image of a single, partially extended R-body. Scale bar = 400 nm. **f,** Schematic indicating planes of view for panels **g** and **h**. **g,** Bright-field and fluorescence microscopy images of three-day-old biofilms formed by the indicated genotypes, containing the P_{rebP1}-*mScarlet* construct. Dotted lines demarcate the edge of the biofilm. Scale bar = 25 mm. **h,** Representative images of thin sections prepared from three-day-old biofilms formed by the indicated genotypes, containing the P_{rebP1}-*mScarlet* construct. Dotted lines denote the interfaces with air (top) and agar (bottom). Scale bar = 10 μm.

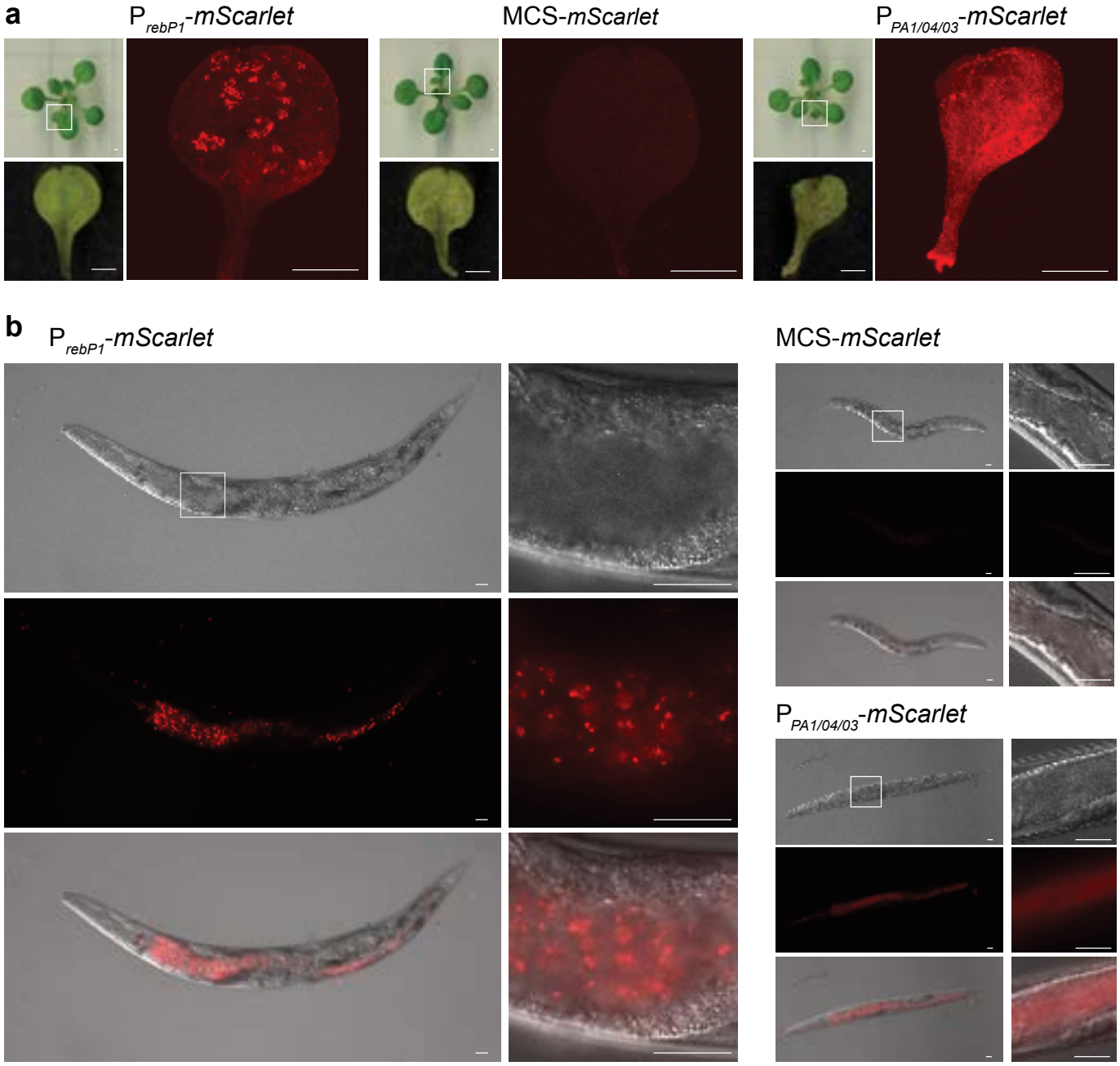

Fig. 2. *rebP1P2* is expressed during host association and contributes to host colonization and killing, but does not confer an advantage during host-independent growth. a, Fluorescent micrographs of *A. thaliana* leaves infected with WT PA14 expressing mScarlet under the control of the *rebP1* promoter (P_{rebP1}-*mScarlet*), no promoter (MCS-*mScarlet*), or a constitutive promoter ($P_{PA1/04/03}$-*mScarlet*). Smaller panels show images of the whole seedling and the imaged leaf indicated by the white box. Images are representative of nine biological replicates from three experiments. Scale bars = 1 mm. **b**, Images of *C. elegans* fed WT PA14 containing the indicated reporter constructs. Top panels, Nomarski; middle panels, fluorescence; bottom panels, overlay. White boxes indicate regions shown in close-up images. Images are representative of 15 replicates from three experiments. Scale bars = 10 μm. **c,** Three-day-old WT and Δ*rebP1P2* biofilms grown on colony morphology medium. Images are representative of nine replicates from three experiments. Scale bar = 4 mm. **d,** Representation of each strain in colony forming units (CFUs) obtained from mixed-strain colony biofilms grown for three days. Error bars represent standard deviation of biological triplicates. **e,** CFUs obtained from *A. thaliana* seedlings inoculated with the indicated genotypes and incubated for five days, normalized to seedling weight. Each circle represents a biological replicate, with color intensity indicating replicates from the same experiment; colored lines indicate means. p-values were calculated using unpaired, two-tailed t-tests. **f,** Killing kinetics of *C. elegans* following exposure to various PA14 genotypes. The role of *gacA* in *C. elegans* pathogenicity has been described previously [30] and *gacA::Tn* therefore serves as a control for defective killing in this assay. Error bars denote standard deviation and p-values were calculated using unpaired, two-tailed t-tests. n ≥ 4 biological replicates from three experiments.